

## Estimation of Monkman-Grant Parameter for Type 316LN and Cr-Mo Stainless Steels

Woo-Gon Kim<sup>\*</sup>, Sung-Ho Kim<sup>\*</sup>, Kyung-Yong Lee<sup>\*\*</sup> and Woo-Seog Ryu<sup>\*</sup>

### 316LN 및 Cr-Mo 스테인리스강의 Monkman-Grant 파라메타 평가

김우곤<sup>\*</sup>, 김성호, 이경용, 류우석

**Key Words:** Monkman-Grant Relation(M-G 관계), Type 316 LN Stainless Steel(316LN 스테인리스강), Cr-Mo Steel(크롬-몰리 강), Steady State Creep Rate(정상상태 크리프속도), Time to Rupture(파단시간)

#### Abstract

The Monkman-Grant (M-G) and its modified parameters were estimated for modified type 316LN and 9-12Cr-1Mo steels with chemical variations. Several sets of creep data were obtained by constant-load creep tests in 550-650°C ranges. The relation parameters,  $m$ ,  $m^*$ ,  $C$  and  $C^*$  were proposed and discussed for two alloy systems. In creep fracture mode, type 316LN steel showed domination of the intergranular fracture caused by growth and coalescence of cavities. On the other hand, the Cr-Mo steel showed transgranular fracture of the ductile type caused from softening at high temperature. In spite of the basic differences in creep fracture modes as well as creep properties, the M-G and its modified relations demonstrated linearity within the  $2\sigma$  standard deviation. The value of the  $m$  parameter of the M-G relation was 0.90 in the 316LN steel and 0.84 in the Cr-Mo steel. The value of the  $m^*$  parameter of the modified relation was 0.94 in the 316LN steel and 0.89 in Cr-Mo steel. The modified relation was superior to the M-G relation because the  $m^*$  slopes almost overlapped regardless of creep testing conditions and chemical variations to the two alloy systems.

#### 1. Introduction

Type 316 austenitic stainless steels are the candidate material for structural components in fast breeder reactor (FBR) because of their good high-temperature mechanical properties. Especially, designed 'LN' grade containing both low carbon (0.03C wt.%) and an appropriate amount of nitrogen (0.1N wt. %) is superior in creep resistance to 'L' grade of low carbon[1-6]. Also, 9-12Cr-1Mo (hereafter Cr-Mo) martensitic stainless steels are the prospective material for nuclear fuel cladding tube, nozzle and flow piping in liquid metal reactor (LMR) because of higher thermal fatigue strength and oxidation resistance than austenitic stainless steels [7-9]. Since these structural components of nuclear

power plants are operated at high temperatures, one of the most critical factors in determining the integrity of their components is creep behavior [10].

In order to design creeping materials, it is essential to achieve reliable long-term test data beyond its design life. However, these long-term data are not available for all of many materials, and to obtain them is time-consuming work and expensive. So, design of creep components can be carried out by extrapolation of short-term creep data to approximate the long-term behavior, if plots of creep data yield reasonable straight lines. Its method is often cheaper and more convenient to conduct stress-rupture tests than long-term creep tests, and it would be very useful if creep strength could be estimated from rupture strength with sufficient accuracy for design purposes. So far, one of the most commonly used methods is known as Monkman and Grant (hereafter M-G) relation [11-12]. It

\* Korea Atomic Energy Research Institute  
Tel : 042-868-2493, E-mail : wkgkim@kaeri.re.kr

\*\* Chung-Ang University

showed empirically that a log-log plot of time to rupture,  $t_r$ , versus steady-state creep rate (or minimum creep rate),  $\dot{\epsilon}_s$ , results in a straight line

$$\log t_r + m \log \dot{\epsilon}_s = C \quad (1)$$

where  $m$  and  $C$  are material parameters. The practical importance of the M-G relation is considerable, if knowing the parameter  $m$  and  $C$ , rupture time can be assessed on the basis of steady state creep rate. This can substantially shorten long-time testing of heat-resistance materials, since the time to reach the secondary stage usually comprises only a small portion of time to rupture.

As a further empirical relation of eqn.(1), the modified relation has been proposed in terms of the total strain at rupture,  $\epsilon_r$ , and new parameters  $m^*$  and  $C^*$ . Eqn.(2) reduces the stress and temperature dependence, introducing the creep strain at rupture [13].

$$\log \left( \frac{t_r}{\epsilon_r} \right) + m^* \log \dot{\epsilon}_s = C^* \quad (2)$$

The exponent  $m^*$  is close to unity and  $C^*$  is temperature independent. Later, the validity of this modified M-G model was found to be in excellent agreement with creep rupture experiments on a few materials; 2.25 Cr-1 Mo steels, martensitic zirconium alloys and 25Cr-20Ni austenitic stainless steel, etc [11-13]. However, as yet, the practical estimation of the M-G and its modified relations for type 316LN and the Cr-Mo stainless steels, which are prospective as candidate materials of FBR and LMR, has not been established by others, and the creep data or the parameters for two alloys are insufficient.

The purpose of this work is to estimate the M-G and its modified parameters for type 316LN and the Cr-Mo stainless steels and to propose their applicability. For this purpose, several sets of creep tests are conducted with chemical variations for the two alloy systems, and creep fracture micrographs are observed to define its fracture

mode related to applicability of the relations.

## 2. Experimental procedures

Laboratory ingots of the 316LN and the Cr-Mo alloys were prepared by vacuum induction melting (VIM), and the chemical compositions for two alloy groups are given in Table 1. Every alloy of the 316LN stainless steel contains around 0.1 wt. % nitrogen instead of 0.03 wt. % low carbon, and each alloy of the Cr-Mo stainless steel is different in minor elements such as vanadium (V), niobium (Nb) and tungsten (W). The ingots were annealed at 1150 °C and for 2 hr in an argon atmosphere and reduced to 15 mm by a hot rolling process. In heat treatment, the 316LN was solution annealed at 1100 °C for 1 hr and water quenched. The Cr-Mo steel was heat treated by normalizing and tempering. Normalizing was held at 1050 °C for 1 hr and air cooled, and tempering at 750 °C for 2 hr and then air cooled.

Creep specimens were taken as the rolling direction and machined to be cylindrical with a 30 mm gage length and 6 mm diameter. The gage sections of the specimens were polished using 1000 grit sand paper with strokes along the specimen axis. Several sets of creep tests were conducted for the 316LN and the Cr-Mo steels using constant-load machines with a 20/1 lever ratio. The test temperature was maintained constantly within  $\pm 2$  °C during the period of the test. Before starting the test, all specimens were held at the test temperature for 1 hr. All creep test procedures were followed according to ASTM standard; E139-83 [14]. Creep data were taken automatically by personal computer or mechanically by the extensometer gage, attached with a precise dial indicator.

After testing, the microstructure for each specimen was examined for fracture surfaces, cavities, and precipitates using scanning electron microscopy (SEM) and optical microscopy (OM). Preparation of the OM specimens is as follows. A small fraction of the crept

specimens was taken from the center part of the gage section along stress axis. And the etching in type 316LN steel followed in mixed solution for 5 minutes ; 10 % hydrochloric acid + 15 % acetic acid + 10% nitric acid + 65 % distilled water and in the Cr-Mo steel followed in the mixed solution for 10 seconds ; 2% hydrofluoric acid + 2% nitric acid + 96% distilled water.

### 3. Results and Discussion

#### 3.1. Creep curves and parameters

Steady-state creep rate and time to rupture data are generally used to analyze or identify deformation processes controlling the creep as a function of the temperature and stress;  $\dot{\epsilon}_s = f(\sigma, T)$  and  $t_r = g(\sigma, T)$ . The dependence of the creep rate on applied stress can be written as power law (or Norton's law) eqn. (3), which can be characterized by the parameter of sensitivity of steady-state creep rate to applied stress,  $n'$  which is defined as eqn. (4).

$$\dot{\epsilon}_s = A \sigma^n \quad (3)$$

$$n' = \left( \frac{\partial \ln \dot{\epsilon}_s}{\partial \ln \sigma} \right)_T \quad (4)$$

Where  $A$  is a constant at a given temperature and  $n$  is stress exponent. For temperature and stress conditions in this work, if using a creep deformation map which illustrated by homologous temperature,  $T/T_m$  and normalized stress regime, the governing deformation of the two alloy systems was corresponded to dislocation creep which yields power law of stress dependence. Such a creep deformation is taken place by movement of dislocation [15-16]. Thus, stress exponent,  $n$  in this work can be written as  $n = n'$ , and it can be optimized by power-law eqn. (3). The  $n$  values of type 316LN alloy groups were investigated to range from 7.3 to 8.0, although a small gap was generated with testing temperatures, stresses, and chemical variations. This

value was similar to the results of  $n = 7.9$  reported by Frost and Ashby in commercial type 316 stainless steel at 650°C [17]. And the  $n$  values of the Cr-Mo martensitic stainless steel were investigated to be greater than 20 at 600°C and 10 at 650°C. Those values among the 9A, 9M, 9MW and 9MN specimens were changed significantly with temperature conditions, that is, the  $n$  value at 650°C was higher than that at 600°C. This means that the creep strength at higher temperature was reduced because the  $n$  value at 650°C decreased. It is believed that thermal stability at high temperature decreased such like microstructures of precipitates and dislocations. The  $n$  exponent has been known as from 4 to 5 typically for dislocation creep in pure metal, and as much greater than 10 in precipitation and dispersion strengthened metallic materials [11,18]. As knowing from the results, the  $n$  value of the Cr-Mo steel was higher than that of the 316LN steel, but its creep rupture time was low inversely.

Figure 1 shows typical creep-rupture curves of type 316LN and the Cr-Mo stainless steels. Creep strain in this figure indicates the different value between creep strain,  $\epsilon_c$  and instantaneous strain,  $\epsilon_p$ . Steady-state creep rates at secondary region as well as total elongation at rupture between two alloy groups were different significantly. Most rupture time in the Cr-Mo steel was occupied with the second stage creep, and its steady-state creep rate was much lower than that of type 316LN stainless steel. However, time to rupture of the Cr-Mo steel was shorter than that of the 316LN steel. This means that the Cr-Mo steel is inferior in creep ductility to the 316LN steel, and most of creep strain was suddenly propagated near to time to rupture. This for the Cr-Mo steel is closely related to material softening at high temperature, which caused by a localized neck of ductile fracture leads to a geometric instability. Thus, two alloy systems are assumed to be some difference in fracture types. The detail discussion for this will be followed in 3.4 section.

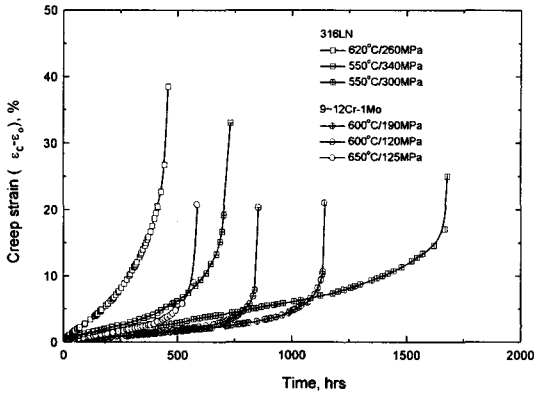


Fig. 1 Typical creep curves for type 316LN and the Cr-Mo stainless steels

### 3.2. The M-G parameters

Figures 2 and 3 show the log-log plot of time to rupture vs. steady-state creep rate for the 316LN and the Cr-Mo steels. The dotted lines represent the  $2\sigma$  standard deviation consisting of 95% prediction upper and lower limits on the basis of time to rupture (y-axis). Solid line in each plot represents a mean value of the  $2\sigma$  standard deviation. By analogy to the linear eqn.(1) of the first order, each plot of the 316LN and the Cr-Mo steels showed linearity within the  $2\sigma$  standard deviation. The  $2\sigma$  standard deviation was 0.12758 in the 316LN steel, and 0.07613 in the Cr-Mo steel. Thus, the  $2\sigma$  standard deviation of the 316LN steel was a wider trend than that of the Cr-Mo steel. This is due to variety in chemical compositions of the 316LN steels (6 kinds) comparing with the Cr-Mo steels (4 kinds), as seen in Table 1.

Figure 4 shows the slope  $m$  curve of time to rupture versus steady-state creep rate for the 316LN and the Cr-Mo steels. Each slope reveals a linear regression for two alloy groups. The  $m$  parameters were found to be a slight difference for two alloy systems, that is,  $m = 0.90$  in the 316LN steel and  $m = 0.84$  in the Cr-Mo steel. Exponent  $m$  has been reported to range about 0.8 to about 0.95 and the parameter  $C$  depends on temperature. Although two alloy systems showed highly different values in the  $n$

or  $\lambda$  parameters due to time to rupture and creep ductility, the  $m$  values of the M-G relation did not vary largely in the reported range. This satisfies clearly the M-G relation regardless of chemical variations to the two alloy systems. In the figure, the steeper slope (higher  $m$  value) means better creep resistance, so the 316LN steel is superior in creep life to the Cr-Mo steel. The computed values of parameters  $m$ ,  $m^*$ ,  $C$ ,  $C^*$  and the  $2\sigma$  standard deviation are given in Table 2.

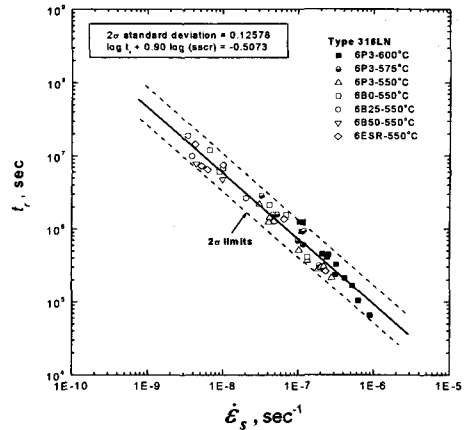


Fig. 2 Rupture time vs. steady state creep rate under different stresses and temperatures for type 316LN stainless steel

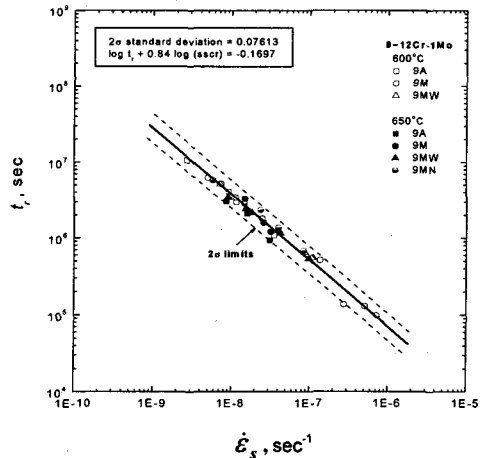


Fig. 3 Rupture time vs. steady-state creep rate under different stresses and temperatures for the Cr-Mo stainless steels

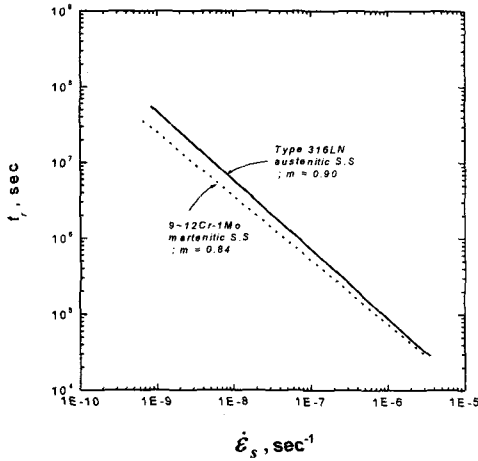


Fig. 4 Comparison of rupture time vs. steady-state creep rate for type 316LN and Cr-Mo stainless steels

### 3.3. Modified M-G parameters

Figures 5 and 6 show the log-log plot of time to rupture over elongation at rupture ( $t_r/\epsilon_r$ ) versus steady-state creep rate for the 316LN and Cr-Mo steels, respectively. Data points fit linearity within scatter band of the  $2\sigma$  standard deviation. In the values of the  $2\sigma$  standard deviation, the 316LN steel was wider because of variety in chemical variations, and the modified relation was higher than that of the M-G relation. However, the values of two relations were approximately similar. In addition, the intercept  $C$  and  $C^*$  values on the M-G and modified relations differ highly between two alloy systems. The  $C^*$  value of the Cr-Mo steel was changed into positive value of 0.1244. This means that rupture elongation of the Cr-Mo steel was relatively lower than that of the 316LN steel.

Figure 7 shows the comparison of the slope  $m^*$  in relation to  $t_r/\epsilon_r$  versus steady-state creep rate for the 316LN and the Cr-Mo steels. For a given creep rate it can be seen in this figure that the 316LN steels have a greater time to rupture than the Cr-Mo martensitic steels. The value of the slope  $m^*$  was 0.94 in the 316LN and 0.89 in the Cr-Mo steel. Such a difference of the slopes obtained for the Cr-Mo martensitic and type 316LN austenitic stainless steels is considered that these two

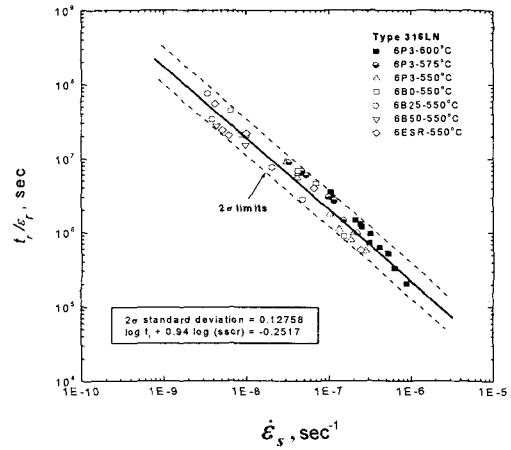


Fig. 5 Modified relation between  $t_r/\epsilon_r$  and  $\dot{\epsilon}_s$  under different stresses and temperatures for type 316LN stainless steel

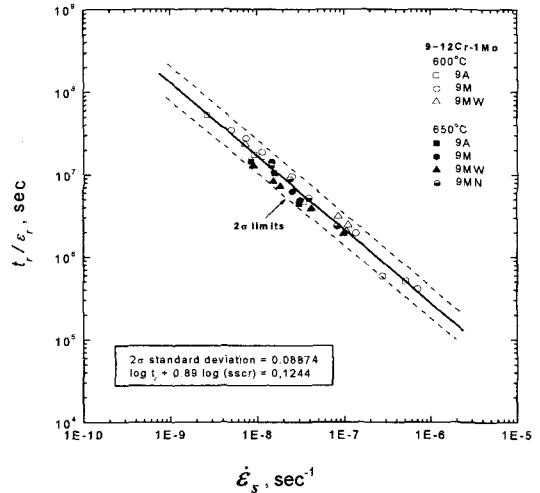


Fig. 6 Modified relation between  $t_r/\epsilon_r$  and  $\dot{\epsilon}_s$  under different stresses and temperatures for the Cr-Mo stainless steel.

alloy systems have the different range of ductility values at fracture and differ mainly in crystal structure. But the  $m^*$  slopes in this figure overlapped nearly regardless of chemical variations as well as testing conditions of two alloy systems. It appears that the parameter  $m^*$  of eqn.(2) clearly demonstrates the superiority over parameter  $m$  of eqn. (1), and also parameter  $m^*$  of eqn. (2) is closer to unity than that of eqn. (1). The reason for this is because the creep elongation at rupture has relation with the

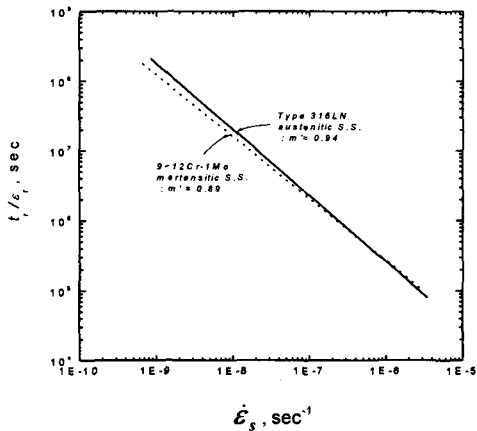


Fig. 7 The log-log plot between  $t_r / \epsilon_r$  and  $\dot{\epsilon}_s$  for type 316LN and the Cr-Mo stainless steels

steady-state creep rate and time to rupture.

In addition, elongation at rupture of 316LN steel showed to be higher than that of the Cr-Mo steel. The data of the elongation at rupture increased with decreasing steady-state creep rate, and main trend of the data depended on the each alloy system, although the relation of the elongation at rupture and steady-state creep rate was a bit of difference with testing conditions or chemical variations. It is therefore believed that the modified relation including the elongation at rupture is a close connection between deformation processes and processes which lead to the formation of cracks and cavities and to final rupture. Furthermore, it means that eqn. (2) indicates typically one process controlling the creep strain during the whole test rather than of various processes predominating at various stages of the creep curve. It is noted that the modified relation is improvement in applicability although the creep properties on the 316LN and the Cr-Mo steels differ basically due to crystal structure.

### 3.4. Creep fracture micrographs

Figures 8 and 9 show the fracture micrographs for the 316LN and the Cr-Mo steels, respectively. The fracture modes of the 316LN and the Cr-Mo stainless steels differ

largely, as shown in (a), (b), and (c) of Figs. 8 (316LN) and 9 (Cr-Mo). Photographs (c) in Figs. 8 and 9 are magnification of fracture surface (b). In the fracture mode, the 316LN showed domination of intergranular fracture, and the crack path propagated along grain boundaries. The fracture was caused from growth and incorporation of cavities. And the cavities were distributed along perpendicular to the stress direction, as seen in Fig. 8(a). On the contrary, the fracture of the Cr-Mo steel showed a transgranular manner of ductile type caused from softening of materials. The cavity cracks were not observed, as seen in Fig. 8(a). Only small size voids were observed at the center of a neck, which axially deformed along the stress direction. Also, reduction of area at its neck was higher than that of the 316LN steel, but the elongation at rupture was inversely. It is noted that the fracture of the Cr-Mo steel was propagated suddenly by softening of material at high temperature without a symptom, and that its fracture mode was ductile type with typical cup-and-cone fracture of a localized necking.

Furthermore, two alloy systems differed basically to morphology of the precipitates in grain boundary, as seen in Figs. 8(d) and 9(d). The precipitates in the 316LN steel were distributed blocky along grain boundaries, which become a nucleation site of cavities or voids. But, the precipitates in the Cr-Mo steel were distributed continuously along lath- or prior-austenitic grain boundaries. These precipitates at higher temperature were changed coarsely and discontinuously by growth and incorporation of them. From the results, it is found that two alloy systems differed basically in creep fracture types as well as creep properties. However, despite these differences, the modified relation of eqn.(2) showed a reliable agreement regardless of creep conditions and chemical variations for the 316LN and Cr-Mo steels, and superiority to the M-G eqn.(1). This agreement in the modified relation is considered because the 316LN steel

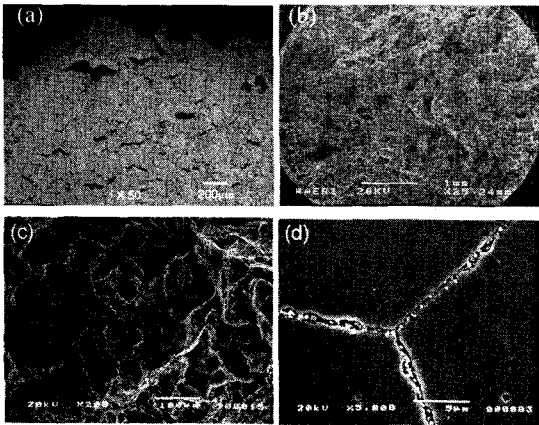


Fig. 8 Typical fracture micrographs of type 316LN stainless steel crept at 300 MPa / 550°C, rupture time is 1679.8 hrs

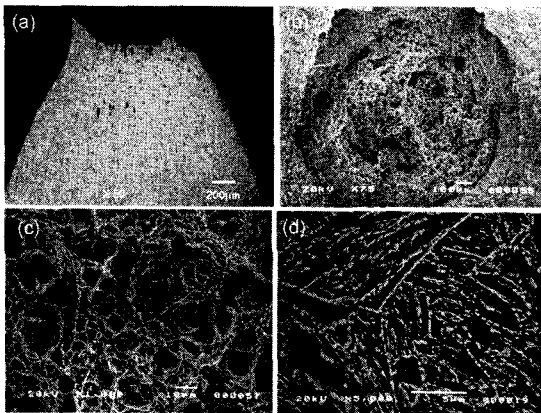


Fig. 9 Typical fracture micrographs of the crept Cr-Mo stainless steel crept at 190 MPa / 600°C, rupture time is 1143.5 hrs

showed intergranular fracture caused by dislocation creep, and because the Cr-Mo steel was relevant to dislocation creep regime at the middle homologous temperature ; about from  $0.40 T_m$  to  $0.44 T_m$  ranges.

#### 4. Conclusions

In order to estimate the M-G and its modified parameters for type 316LN and Cr-Mo stainless steels, several sets of laboratory ingots were prepared with chemical variations. Creep data for the two alloy systems were obtained by constant-load creep tests in 550-650°C

ranges. In creep fracture mode, type 316LN steel showed domination of the intergranular fracture caused by growth and coalescence of cavities. On the other hand, the Cr-Mo steel showed the transgranular fracture of ductile type caused by softening of materials at high temperature. In spite of these differences in creep fracture modes as well as creep properties, these relations demonstrated linearity within the  $2\sigma$  standard deviation regardless of creep testing conditions and chemical variations. The value of the  $m$  parameter of the M-G relation was found to be a slight difference for two alloy systems, such as  $m = 0.90$  in the 316LN steel and  $m = 0.84$  in the Cr-Mo steel. Also, the value of the  $m^*$  parameter of the modified relation was 0.94 in the 316LN steel and 0.89 in the Cr-Mo steel. Thus, type 316LN austenitic stainless steel existed a greater rupture time than do the Cr-Mo martensitic stainless steel. Such differences of the  $m$  and  $m^*$  parameters are due to ductility values at fracture and crystal structures. It was found that the modified relation was superior to the M-G relation because the  $m^*$  slopes almost overlapped regardless of the two alloy systems.

#### Acknowledgements

This work is a part of the Nuclear Material Development Project, which has been financially supported by the Korean Ministry of Science and Technology.

#### References

- (1) W. S. Ryu and W. G. Kim, 1988, *KAERI/AR-487*, p. 37.
- (2) Y. J. Oh and J. H. Hong, 1998, *J. of Nuclear Materials* Vol. 278, p. 242.
- (3) T. Nakazawa, 1988, *HNS 88*, p. 218.
- (4) J. K. Solber, 1982, *Materials Science and Engineering*, Vol. 55, p. 39.
- (5) E. Manfredi and E. Vitale, 1984, Proc. of the 2nd International Conference on Fracture of Engineering Materials and Structures, Edited by B. Wilshire and D.R.J. Owen , Pineridge Press, Swansea, p. 1239.

- (6) M. Fujiwara, H. Uchida, S. Ohta, S. Yuhara, S. Tani and Y. Sato, 1986, *ASTMSTP 955*, p. 127.
- (7) H. Berns and F. Krafft, 1990, Proc. of the Conf. on Rupture Ductility of Creep Resistance Steels, edited by A. Strang, p.116.
- (8) P. F. Aplin, C. K. Bullough and D. J. Barlow, 1990, Proc. of the Conf. on Rupture Ductility of Creep Resistance Steels, Edited by A. Strang, p.125.
- (9) W. G. Kim and W. S. Ryu, 2000, *2000KSME 00MF078*, p. 232.
- (10) R. Viswanathan, 1989, "Damage Mechanisms and Life Assessment of High-Temperature Components", *ASM International*, p. 10.
- (11) J. Cadek, 1988, "Creep in Metallic Materials", p. 335.
- (12) F. R. N. Nabarro and H. L. Villers, 1995, "The Physics of Creep", p. 22.
- (13) F. Dobes and K. Millicka, 1976, *Metal Science*, Vol. 10, p. 382.
- (14) *ASTM E139-83*, 1988, p.305.
- (15) W. G. Kim, D. W. Kim and W. S. Ryu, 2000, *J. of the KSME*, Vol. 24, p. 2326.
- (16) R. K. Penny and D. L. Marroott, 1995, "Design for Creep," 2nd edition-Champan & Hall, p. 141.
- (17) H. Riedel, 1987, "Fracture at High Temperature", MRE Springer-Verlag, p. 390.
- (18) R. W. Evans and B. Wilshire, 1985, "Creep of Metals and Alloys", p. 9.

Table 1 Chemical compositions of modified type 316LN and 9~12Cr-1Mo stainless steels(wt.%)

Elements		C	Si	Mn	P	S	Cr	Ni	Mo	N	B	V	Nb	W
316LN steel	6P3	0.019	0.64	0.97	0.002~0.018	0.006	17.25	12.41	2.39	0.10	-	-	-	-
	6ESR	0.026	0.70	0.97	0.010	0.001	17.35	12.40	2.39	0.10	-	-	-	-
	6B0	0.021	0.70	0.97	0.021	0.006	17.30	12.34	2.36	0.10	-	-	-	-
	6B25	0.023	0.67	0.96	0.020	0.006	17.28	12.43	2.38	0.10	0.0025	-	-	-
	6B50	0.023	0.63	0.97	0.025	0.005	17.27	12.45	2.34	0.09	0.0050	-	-	-
9~12% Cr-1Mo steel	9A	0.19	0.10	0.59	0.019	0.006	11.79	0.53	0.99	<0.01	-	0.310	0.020	0.450
	9M	0.15	0.08	0.48	0.002	0.004	9.94	0.49	1.27	0.02	-	0.203	0.195	-
	9MW	0.18	0.09	0.47	0.002	0.004	9.87	0.42	0.49	0.02	-	0.202	0.203	0.201
	9MN	0.15	0.08	0.48	0.002	0.004	10.00	0.50	1.28	0.045	-	0.205	0.204	-

Table 2 Summary of test values and equation constants

Alloy systems	Experimental values		M-G relation(eq.1)			Modified relation (eq. 2)		
	Temp. range, °C	Number of points	M	C	2σ	m*	C*	2σ
316LN	550-600	49 points	0.90	-0.5073	0.12758	0.94	-0.2517	0.14204
9~12% Cr-Mo	600-650	32 points	0.84	-0.1697	0.07613	0.89	+0.1244	0.08874